Presenilin-Dependent γ-Secretase on Plasma Membrane and Endosomes Is Functionally Distinct†

Akio Fukumori,‡,§ Masayasu Okochi,*,‡,§ Shinji Tagami,‡,§ Jingwei Jiang,§ Naohiro Itoh,§ Taisuke Nakayama,§ Kanta Yanagida,§ Yoshiko Ishizuka-Katsura,§ Takashi Morihara,§ Kojin Kamino,§ Toshihisa Tanaka,§ Takashi Kudo,§ Hisashi Tanii,§ Akiko Ikuta,§ Christian Haass,|| and Masatoshi Takeda§

Division of Psychiatry and Behavioral Proteomics, Department of Post-Genomics and Diseases, Osaka University Graduate School of Medicine, Osaka, Japan, and Adolf Butenandt Institute, Department of Biochemistry, Laboratory for Alzheimer's and Parkinson's Disease Research, Ludwig-Maximilians University, Munich, Germany

Received November 25, 2005; Revised Manuscript Received February 25, 2006

ABSTRACT: The presenilin (PS)/γ-secretase complex, which contains not only PS but also Aph-1, PEN-2, and nicastrin, mediates proteolysis of the transmembrane domain of β-amyloid protein precursor (βAPP). Intramembrane proteolysis occurs at the interface between the membrane and cytosol (ε-site) and near the middle of the transmembrane domain (γ-site), generating the βAPP intracellular domain (AICD) and Alzheimer disease-associated Aβ, respectively. Both cleavage sites exhibit some diversity. Changes in the precision of γ-cleavage, which potentially results in secretion of pathogenic Aβ42, have been intensively studied, while those of ε-cleavage have not. Although a number of PS-associated factors have been identified, it is unclear whether any of them physiologically regulate the precision of cleavage by PS/γ-secretase. Moreover, there is currently no clear evidence of whether PS/γ-secretase function differs according to the subcellular site. Here, we show that endocytosis affects the precision of PS-dependent ε-cleavage in cell culture. Relative production of longer AICDε49 increases on the plasma membrane, whereas that of shorter AICDε51 increases on endosomes; however, this occurs without a concomitant major change in the precision of cleavage at γ-sites. Moreover, very similar changes in the precision of ε-cleavage are induced by alteration of the pH. Our findings demonstrate that the precision of ε-cleavage by PS/γ-secretase changes depending upon the conditions and the subcellular location. These results suggest that the precision of cleavage by the PS/γ-secretase complex may be physiologically regulated by the subcellular location and conditions.

Intramembrane proteolysis by presenilin (PS)/γ-secretase plays a key role in both Alzheimer disease (AD)[1] and regulated intramembrane proteolysis (RIP) signaling (*1*). At least two PS-dependent cleavages occur in the transmembrane domains of substrates such as β-amyloid protein precursor (βAPP), Notch, and CD44 ("dual cleavage"): one near the middle of the transmembrane domain (TM-N) (*2*−*5*) and the other on the border between the transmembrane domain and cytosol (TM-C) (*6*−*10*). The cleavage at the TM-N site of βAPP (γ-cleavage) is essential for Aβ generation and is closely related to AD (*2*, *11*). On the other hand, the cleavage at the TM-C site, including that in Notch-1 (S3-cleavage), generates ICDs (*i*ntracellular *c*ytoplasmic *d*omains) and is involved in RIP signaling (*1*).

In PS-dependent proteolysis, there is some diversity in the specific sites of cleavage (*3*, *5*, *7*−*9*, *11*). A change in cleavage precision can have an important effect on the pathogenesis of AD because Aβ42, a causative factor in AD, is generated by one of the types of γ-cleavage (*2*, *11*). Much time and effort have therefore been dedicated to understanding how the precise site of cleavage is determined. Most familial AD-associated PS and βAPP mutants affect the precision of γ-cleavage (*11*). Because such changes in the precision of γ-cleavage have not been observed in other conditions, it had been generally believed that the precision of this cleavage is not easily changed (*11*). Recent studies, however, have revealed that some chemicals including NSAIDs (*n*on*s*teroidal *a*nti*i*nflammatory *d*rug*s*) (*12*, *13*) up- or downregulate pathological Aβ42, indicating that the precision of this cleavage by PS/γ-secretase may change under certain circumstances (*14*). Notably, however, corresponding changes in the precision of ε-cleavage have not been examined.

ICDs including that of βAPP (AICD) and Notch (NICD) are generated by ε- and S3-cleavage at TM-C, respectively (*1*). ICDs are generally involved in translocation of signaling

† This work was supported by the Program for the Promotion of Fundamental Studies in Health Sciences of the National Institute of Biomedical Innovation (05-26), by Grants-in-Aid for Scientific Research on Priority Areas−Advanced Brain Science Project and for KAKENHI from the Ministry of Education, Culture, Sports, Science, and Technology of Japan, and by Grants-in-Aid from the Ministry of Health, Labor, and Welfare of Japan.

* To whom correspondence should be addressed. Tel: 81-6-6879-3053. Fax: 81-6-6879-3059. E-mail: mokochi@psy.med.osaka-u.ac.jp.

‡ Equal contributions.

§ Osaka University Graduate School of Medicine.

|| Ludwig-Maximilians University.

[1] Abbreviations: Aβ, amyloid-β peptide; AD, Alzheimer disease; AICD, βAPP intracellular cytoplasmic domain; βAPP, β-amyloid protein precursor; CMF, crude membrane fraction; CTF, carboxyl-terminal fragment; Dyn-1, dynamin-1; IP-MS, immunoprecipitation−mass spectroscopy; K293, human embryonic kidney 293; PM, plasma membrane; PS, presenilin; sw, Swedish mutant; TM-C, the border between the transmembrane domain and cytosol.

10.1021/bi052412w CCC: $33.50
Published on Web 03/28/2006

molecules to the nucleus to activate target genes in RIP signaling (*1*). Although, like γ-cleavage, ϵ-cleavage also exhibits diversity (*7*−*9*), the details of this diversity and the characteristics of the cleavage remain to be clarified. Both ϵ- and γ-cleavages are mediated by PS/γ-secretase (*2*), but whether the processes that determine the variety and the precision of these cleavages are common remains controversial. For example, it has been shown that ϵ-cleavage sites are associated with γ-cleavage sites (*7*, *15*, *16*); however, mutagenesis studies show that ϵ- and γ-cleavages are mediated by a distinct process (*17*).

PS is the proteolytic active center in the PS/γ-secretase protein complex (*2*, *18*). To exert its proteolytic function, PS must form a complex with at least nicastrin (*19*), PEN-2 (*20*), and APH-1 (*2*, *20*). Other factors that physiologically affect proteolysis, including the precision of cleavage, have not yet been identified. In contrast to other subcellular locations, AD-associated Aβ42 is produced in the ER without concomitant production of Aβ40. However, since this is not mediated by PS (*21*, *22*), whether the precision of PS-dependent proteolysis changes within cells depending on location or conditions remains unresolved.

In this study, using a cell-free γ-secretase assay, we examined whether the precision of cleavage by PS/γ-secretase is affected by its subcellular location. We demonstrate that, unlike γ-cleavage, ϵ-cleavage precision can drastically change depending on subcellular location and the pH. Relative cleavage at the ϵ51 site is more prone to occur on endosomes than on plasma membrane (PM) and at lower pH. In contrast, relative cleavage at the ϵ49 site is more likely to occur on PM than on endosomes and at higher pH. These results suggest that PS-dependent γ-secretase on plasma membrane and endosomes is functionally distinct.

MATERIALS AND METHODS

Antibodies. Rabbit antiserum 6618 was raised against a synthetic peptide KMQQNGYENPTYKFFEQMQN, which corresponds to the C-terminus of βAPP according to the methods described (*23*). The following antibodies were purchased from commercial sources: anti-Aβ antibody 4G8 (Senetec PLC), anti-Na−K ATPase (Upstate Biotechnology), anti-early endosome antigen 1 (BD Transduction Laboratories), anti-nicastrin (Sigma-Aldrich), anti-GM130 (BD Transduction Laboratories), and anti-tubulin (Santa Cruz Biotechnology). Also, antibody 12CA5 (Roche Diagnostics Inc.) was used to detect the N-terminal hemagglutinin-tagged dynamin-1 (Dyn-1) K44A mutant.

Cell Culture and cDNA Construct. Human embryonic kidney 293 (K293) cells stably expressing wild-type βAPP, wild-type PS1/βAPP Swedish (sw) mutant (*24*), or PS1 D385N/βAPP sw (*25*) were described previously. HeLa cells expressing Dyn-1 K44A under control of a tetracycline transactivator were kindly provided by Dr. Sandra L. Schmid (Scripps Institute, La Jolla, CA) (*26*). HeLa cells stably expressing βAPP sw were cultured without tetracycline (Sigma-Aldrich) for 48 h to induce expression of Dyn-1 K44A.

Membrane Fractionation and Cell-Free γ-Secretase Assay. The collected cells were homogenized with a Teflon homogenizer (20 strokes) in homogenization buffer (0.25 M sucrose and 10 mM HEPES, pH 7.4) containing a protease inhibitor cocktail (Roche) (*27*). The homogenate was centrifuged at 1000*g* for 5 min to remove nuclei and cell debris, followed by further centrifugation of the supernatant fraction at 100000*g* for 1 h. Following a single wash with homogenization buffer, the resulting precipitate was collected as the CMF and frozen in liquid nitrogen. Upon use, the frozen CMF samples were resuspended and immediately incubated in the reaction buffer [150 mM sodium citrate buffer (pH 5.0−7.4) containing 5 mM 1,10-phenanthroline (Sigma-Aldrich) and a 4× concentration of protease inhibitor cocktail (Roche)] for 20 min at 37 °C (cell-free incubation) (*28*, *29*). The reaction was terminated by placing the samples on ice.

Subcellular Fractionation. Linear gradients of 2.5−25% iodixanol (Optiprep; AXIS-SHIELD) were prepared. Postnuclear supernatant fractions from 24 dishes (ϕ = 14 cm) were loaded on the top of the gradient, followed by centrifugation for 3 h at 130000*g*. Each fraction was diluted with three volumes of homogenization buffer and centrifuged for 1 h at 100000*g* to precipitate the membranes. The precipitated membrane was used in cell-free γ-secretase assays or in immunoblots for marker proteins.

Metabolic Labeling. Following methionine starvation for 40 min, cells were metabolically labeled with 400 μCi of [^{35}S]methionine (Redivue Promix; Amersham Pharmacia Biotech) in methionine-free MEM for 20 min and chased for 30 min in DMEM containing 10% FBS and excess unlabeled methionine.

Immunoprecipitation/Autoradiography Analysis. Metabolically labeled CMF was lysed in RIPA buffer (1% Triton X-100, 0.5% sodium deoxycholate, and 0.1% SDS) containing a protease inhibitor mix (Sigma-Aldrich). The cell lysates were centrifuged at 10000*g* for 15 min, and the supernatant fractions were immunoprecipitated with 6618 antiserum for the detection of the C-terminal stub and de novo AICD. Following 10−20% Tris−tricine SDS−PAGE (Invitrogen), the gels were dried and analyzed by autoradiography (*3*).

Immunoprecipitation/Mass Spectroscopy (IP-MS) Analysis. IP-MS analysis was carried out as described previously (*3*). Following cell-free incubation, the CMF was sonicated four times for 10 s and then centrifuged at 100000*g* for 1 h. The supernatant were immunoprecipitated for 4 h at 4 °C in IP-MS buffer [140 mM NaCl, 0.1% *n*-octyl glucoside, 10 mM Tris-HCl (pH 8.0), 5 mM EDTA, and a protease inhibitor mix (Sigma-Aldrich)]. The heights of the MS peaks and molecular weights were calibrated using ubiquitin and/or bovine insulin β-chain as standards (Sigma-Aldrich). The relative peak heights were semiquantitatively analyzed (see Figure 3 in Supporting Information).

Immunoprecipitation/Immunoblot Analysis. Following cell-free incubation, the fractions were immunoprecipitated for 10 h at 4 °C in IP-MS buffer. After SDS−PAGE, the separated proteins were transferred to a PVDF or nitrocellulose (for detection of Aβ) membrane and probed with the indicated antibodies (*30*). The nitrocellulose membrane was heated for 10 min in boiling PBS before blocking. AICD and Aβ levels were semiquantified by chemiluminescence using an LAS3000 scanner and Multi Gauge Ver3.0 software (Fujifilm).

Transferrin Uptake Assay. To determine the level of internalized transferrin, the treated cells were washed three times in Hank's balanced salt solution (Sigma-Aldrich), pH 7.4, and then treated for 7 min at 37 °C with 8 μg/mL biotin−

transferrin (Sigma-Aldrich) in conditioned medium. To remove remaining surface-bound biotin−transferrin, cells were washed three times with Hank's balanced salt solution, pH 4.0. To determine the level of surface-bound transferrin, the treated cells were incubated for 30 min with biotin−transferrin at 4 °C and washed three times with Hank's balanced salt solution, pH 7.4 (*26*). The resulting cell lysates were separated by SDS−PAGE and transferred to the PVDF membrane. Biotin−transferrin was detected by neutravidin−horseradish peroxidase (Pierce). The level of endocytosis in each condition was expressed as of the ratio of internalized vs surface-bound transferrin (*31*).

RESULTS

The Cell-Free Assay Constitutes Bona Fide ϵ- and γ-Cleavages by PS/γ-Secretase. βAPP, a type 1 transmembrane protein, undergoes PS-dependent proteolysis in its transmembrane domain, following "shedding" of the extracellular domain at β- or α-sites (*11*). The intramembrane proteolysis is composed of at least two distinct proteolytic cleavages (dual cleavage), namely, at the ϵ- and γ-sites (Figure 1A) (*2*).

To determine whether the precision of cleavage in intramembrane proteolysis by each PS/γ-secretase is homogeneous in cells, we established a cell-free γ-secretase assay using a detergent-free membrane fraction (Figure 1) (*28*). First, de novo AICD generation from carboxyl-terminal fragment (CTF) stubs of βAPP was analyzed (Figure 1B,C). Following a 20 min metabolic labeling of K293 cells stably expressing βAPP sw and a 30 min chase, we extracted CMFs from the cells and incubated them under various conditions (cell-free incubation). To detect the C-terminus of βAPP, cell lysates were immunoprecipitated with rabbit antiserum 6618, separated by SDS−PAGE, and analyzed by autoradiography. As shown in Figure 1B, during cell-free incubation of the purified CMF, radiolabeled CTF stubs of βAPP rapidly underwent endoproteolysis and concomitantly generated labeled AICD. Termination of the PS function by either exogenous expression of the PS1 dominant negative mutant (D385N) (*32*) or by addition of a specific γ-secretase inhibitor to CMF (Figure 1C) inhibited generation of AICD.

We next examined the precision of both ϵ- and γ-cleavages in the cell-free assay using IP-MS analysis (Figure 1D). We first examined the molecular species of AICD generated during cell-free incubation. The IP-MS analysis showed that the MS profile of AICD was consistent with that previously reported (Figure 1D, left panel) (*7*−*9*). In addition, the MS spectrum of Aβ generated during cell-free incubation (Figure 1D, right panel) was almost identical to that of Aβ present in the conditioned medium just before extraction of the CMF (data not shown). We therefore conclude that the cleavages in the cell-free assay constitute bona fide PS-dependent ϵ- and γ-cleavages (Figure 1E).

The Precision of ϵ-Cleavage Drastically Changes upon Inhibition of Endocytosis. Proteolysis by PS/γ-secretase occurs on cell organelles including the PM and endosomes before and after endocytosis (*33*). Here, we focused on whether the precision of ϵ- and γ-cleavage changes upon inhibition of endocytosis. To inhibit endocytosis, we used the "tet-off system" (Clontech) in which the expression of the dynamin-1 (Dyn-1) dominant negative mutant K44A is

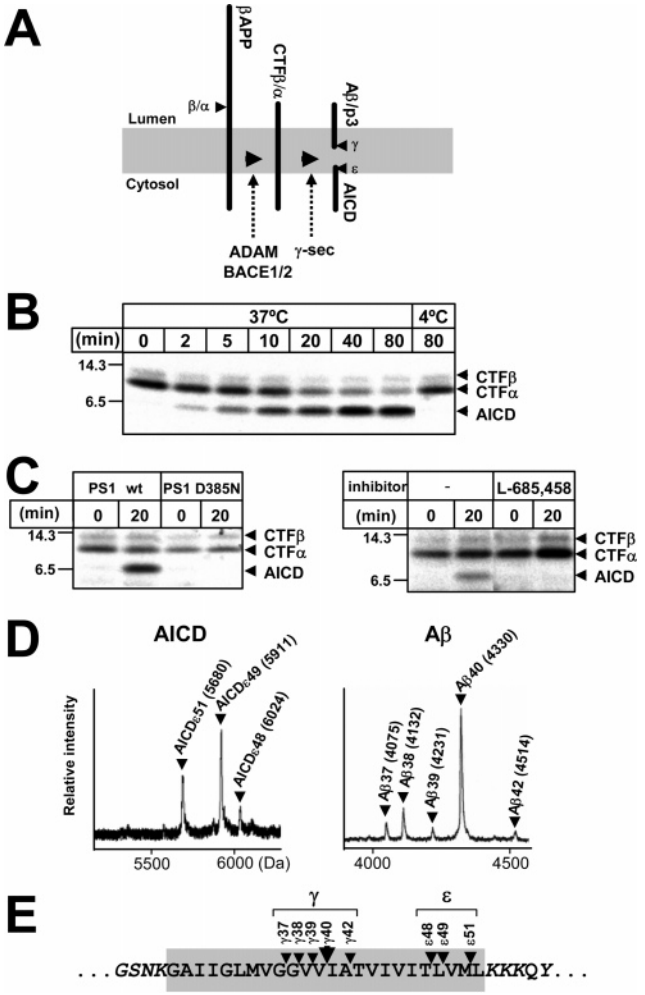

FIGURE 1: Generation of de novo AICD and Aβ in the cell-free γ-secretase assay. (A) Schematic representation of dual cleavage of the βAPP transmembrane domain. See Results for details. (B) Analysis of cell-free γ-secretase assay products by immunoprecipitation/autoradiography using CMF from cells stably expressing βAPP sw. Note that the ~7 kDa product (AICD) was generated over time along with a concurrent reduction in the level of substrates (CTF stubs of βAPP). (C) Analysis of cell-free γ-secretase assay products by immunoprecipitation/autoradiography using CMFs from (i) cells expressing a dominant negative PS1 mutant (PS1 D385N) or (ii) cells treated with or without 10 μM L685,458. (D) Molecular species of de novo AICD and Aβ generated in the cell-free assay. Molecular weights of de novo AICD (left panel) and Aβ (right panel) are shown. Following a 20 min cell-free incubation, the soluble fraction of CMF was immunoprecipitated with antibody 6618 (left panel) or 4G8 (right panel). Panels B−D show representative data from more than three independent experiments. (E) Schematic representation of the ϵ- and γ-cleavages of βAPP. Arrowheads indicate the cleavage sites found in the assay.

induced by tetracycline withdrawal (tet (−) treatment) in HeLa cells (Figure 2A) (*26*). We first examined the extent to which this mutant suppresses endocytosis of the transferrin receptor. We found that expression of Dyn-1 K44A inhibited the intracellular uptake of biotinylated transferrin (Figure 1 in Supporting Information) by approximately 87 ± 2% (Figure 2B).

Next, we analyzed the ϵ-cleavage in the cell-free γ-secretase assay using CMF from cells cultured with or without tetracycline (Figure 2C,D). Unlike the analysis of K293 cells, the mass spectral analysis showed that AICDϵ51 was a major species formed by CMF from HeLa cells stably expressing

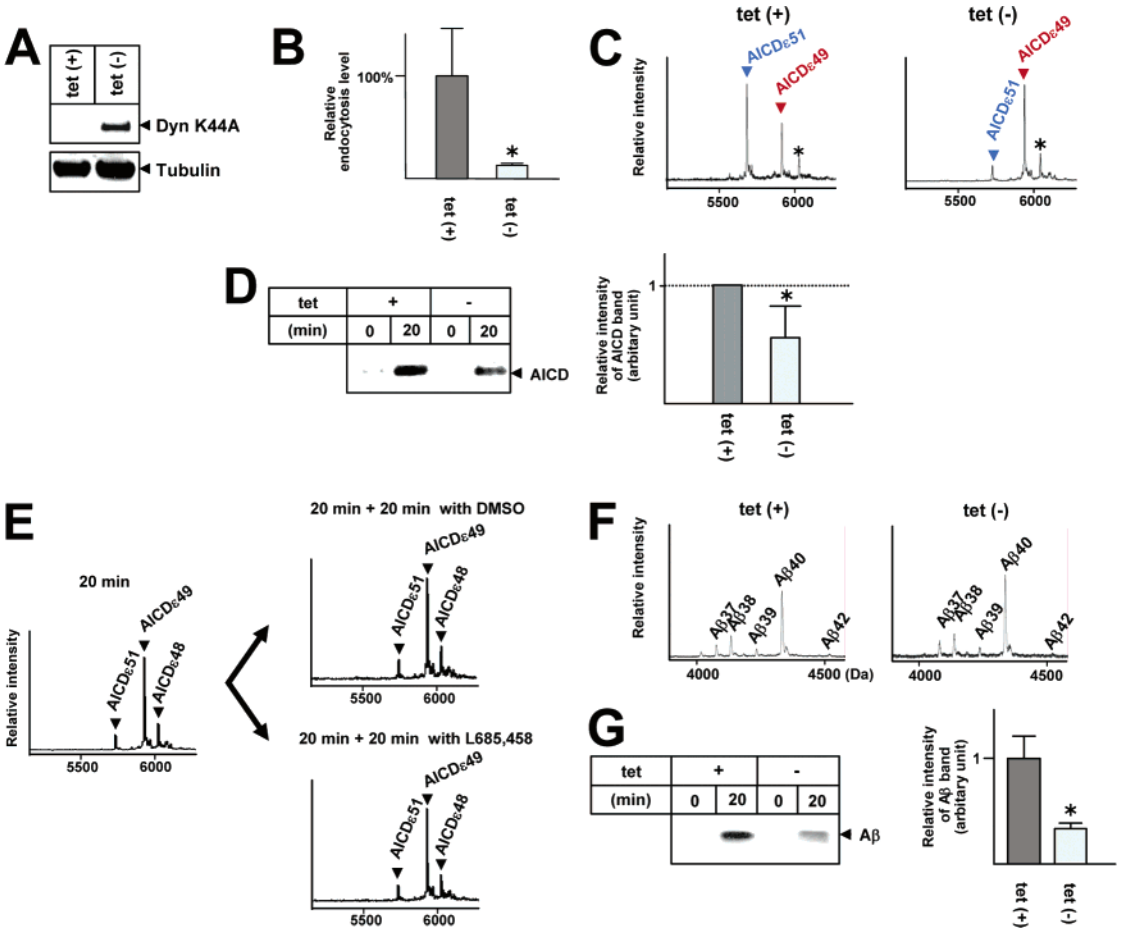

FIGURE 2: Effects of Dyn-1 K44A expression in HeLa cells on the cell-free γ-secretase assay. (A) Induction of Dyn-1 K44A expression. Cells were treated without (−) or with (+) tetracycline, and cell lysates were immunoblotted with 12CA5 (upper panel) or anti-tubulin (lower panel). The results show that Dyn-1 K44A is induced by removal of tetracycline. (B) Inhibition of endocytosis by Dyn-1 K44A expression. The ratio of internalized transferrin at 37 °C to cell surface bound transferrin at 4 °C in cells not expressing Dyn-1 K44A (tet(+)) was defined as 100%. The ratio of endocytosis decreased to 13 ± 2% when the expression of the mutant was induced (tet(−)). The asterisk indicates statistical significance ($P < 0.05$ by Student's *t*-test). (C) Mass spectra of cell-free generated AICD species. The CMFs from HeLa cells expressing βAPP sw cultured with or without tetracycline were incubated in the cell-free assay. Asterisks indicate the AICDϵ48 species. (D) The level of AICDs generated in the cell-free assay. The AICDs generated in cell-free assays were immunoprecipitated and immunoblotted with the 6618 antiserum (left panel). The intensity of each AICD band was measured by chemiluminescence (right panel). Generation of de novo AICDs was defined as the difference of the AICD band intensities with or without a 20 min cell-free incubation. The asterisk indicates statistical significance ($P < 0.01$ by Student's *t*-test). (E) Molecular species of AICD observed after a first (left panel) and a second 20 min incubation with L685,458 (lower right panel) or vehicle control DMSO (upper right panel) using CMF from HeLa cells expressing βAPP sw cultured without tetracycline. (F) Mass spectra of the Aβ species generated in the cell-free reaction. The samples were the same as those analyzed in panel C. (G) The level of Aβ produced in the cell-free assay. The Aβ generated in the cell-free assay was analyzed by immunoprecipitation, followed by immunoblotting with the 4G8 antibody (left panel). The intensity of each Aβ band was measured by chemiluminescence (right panel). The asterisk indicates statistical significance ($P < 0.01$ by Student's *t*-test). In (A), (C), (E), and (F) and in the left panels of (D) and (G), the results are representative data of more than three independent experiments. The results in (B) and the right panels of (D) and (G) indicate the means ± standard deviations of at least triplicate determinations. tet = tetracycline.

βAPP sw in our cell-free assay (Figure 2C, left panel, and Figure 3A, right panel). Surprisingly, expression of Dyn-1 K44A greatly increased the peak height of AICDϵ49 relative to that of AICDϵ51, indicating a change in the precision of ϵ-cleavage upon inhibition of endocytosis (Figure 2C; see also Table 1). A very similar large relative increase of the peak height of AICDϵ49 compared to that of AICDϵ51 was also observed upon addition of 100 nM bafilomycin A1 (Figure 2B in Supporting Information), which inhibited endocytosis by approximately 69 ± 5% (Figures 1 and 2A in Supporting Information) (*34*). Moreover, we found that the relative ratio of the AICDϵ49 peak height to that of AICDϵ51 semiquantitatively correlated with the relative amount of each AICDϵ49 species, indicating that AICDϵ49 and AICDϵ51 have similar ionization efficiencies in the matrix-associated laser desorption ionization/time-of-flight mass spectrometry (see Figure 3 in Supporting Information). We also examined whether the level of ϵ-cleavage changes upon inhibition of endocytosis by immunoblotting (Figure 2D). We detected a significant decrease in intensity of the AICD band upon Dyn-1 K44A expression, indicating that the level of ϵ-cleavage decreases upon inhibition of endocytosis. These findings suggest that inhibition of endocytosis causes a drastic change in the precision of ϵ-cleavage.

We further investigated whether both AICDϵ51 and AICDϵ49 are, indeed, direct products of PS/γ-secretase. We first generated de novo AICD by a 20 min cell-free incubation (Figure 2E, left panel). The solution was further incubated for 20 min with (Figure 2E, lower right panel) or without (Figure 2E, upper right panel) the γ-secretase

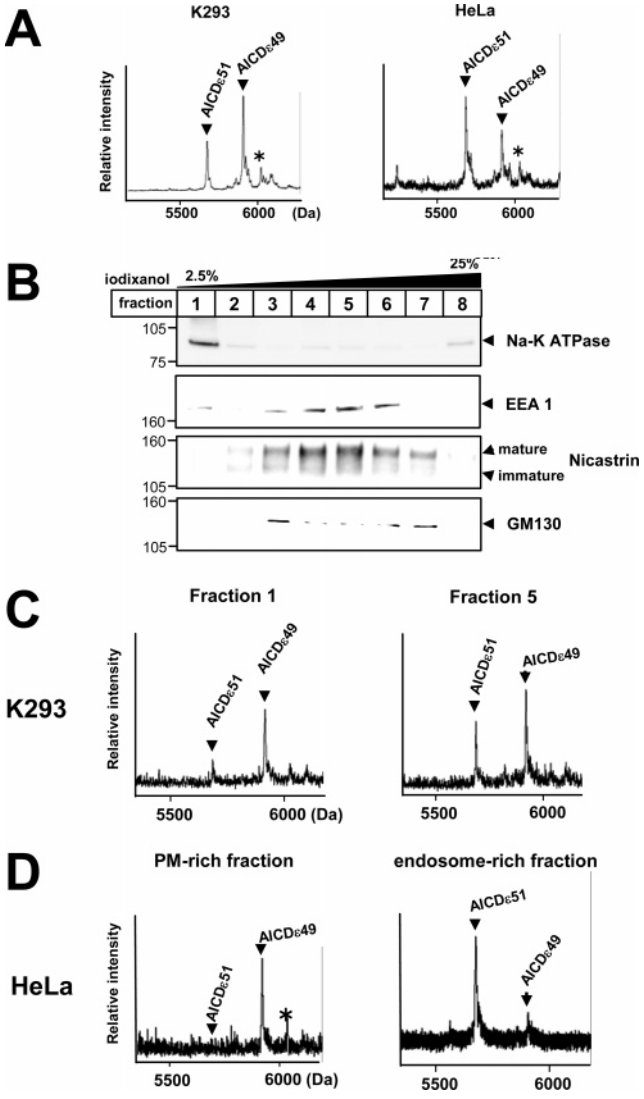

FIGURE 3: Cell-free γ-secretase assay using PM- and endosome-rich fractions. (A) Mass spectra of de novo AICD generated in the cell-free assay using whole CMFs from K293 (left panel) and HeLa (right panel) cells. Asterisks indicate AICDϵ48 species. (B) Postnuclear supernatant fractions of βAPP sw-expressing K293 cells were separated by iodixanol gradient centrifugation and analyzed by immunoblotting using antibodies to organelle marker proteins. (C) Mass spectra of de novo AICD generated by fractions 1 and 5 from K293 cells. (D) Mass spectra of de novo AICD generated by PM- or endosome-rich fractions from HeLa cells expressing βAPP sw. Results in (A) to (D) are representative of more than three independent experiments.

inhibitor L685,458. This inhibitor neither increased the relative peak height of AICDϵ51 nor reduced that of AICDϵ49/AICDϵ48, suggesting that AICDϵ51 is not a degradation product of AICDϵ49/AICDϵ48 but rather is generated directly by PS/γ-secretase.

These results indicated that there is a striking change in the precision of ϵ-cleavage upon inhibition of endocytosis. We therefore examined whether there is also a parallel remarkable change in the precision of γ-cleavage. We chose IP-MS analysis in order to observe all of the de novo Aβ species. In clear contrast to the analysis of AICD (Figure 2C), IP-MS analysis did not reveal drastic differences in the profiles of de novo Aβ species (i.e., Aβ37, Aβ38, Aβ39, Aβ40, and Aβ42) between reactions using CMF from control cells (Figure 2F, left panel) and cells expressing Dyn-1 K44A (Figure 2F, right panel). Also, very similar results were observed upon inhibition of endocytosis by bafilomycin A1 (Figure 2C in Supporting Information). Immunoprecipitation/immunoblotting analysis for detecting Aβ species revealed a significant decrease upon expression of Dyn-1 K44A (Figure 2G). Thus, in parallel to AICD, we detected a decrease in the level of de novo Aβ levels in the presence of Dyn-1 K44A expression. These results indicated a concomitant decrease in both ϵ- and γ-cleavage efficiencies by PS/γ-secretase upon inhibition of endocytosis.

The Precision of ϵ-Cleavage in the PM-Rich Fractions Is Distinct from That in the Endosome-Rich Fractions. Our cell-free γ-secretase assay revealed that inhibition of endocytosis by expression of the Dyn-1 K44A mutant causes a drastic change in the precision of ϵ-cleavage by PS/γ-secretase but does not concurrently cause such a change in the precision of γ-cleavage. This prompted us to investigate whether there are differences in the precision of ϵ-cleavage on the PM and endosomes. Using CMFs from K293 and HeLa cells, we performed cell-free γ-secretase assays and examined the mass spectra of the generated AICD. As described above (Figures 1D and 2C), in unstimulated K293 and HeLa cells, the relative amounts of ϵ49 and ϵ51 produced are different, indicating that the precision of cleavage at the ϵ-site is distinct in the two cell lines (Figure 3A).

We next examined the production of AICD species in PM- and endosome-rich fractions isolated by iodixanol density gradient centrifugation from CMF prepared from K293 cells expressing βAPP sw. Na−K ATPase, a marker of PM, was detected primarily in the lightest fraction (fraction 1; Figure 3B, first panel), whereas the early endosome markers early endosome antigen 1 (Figure 3B, second panel) and matured nicastrin (Figure 3B, third panel) were detected together in higher density fractions (fractions 4 and 5). GM130, a marker of Golgi, was found mainly in fractions 3 and 7 (Figure 3B, fourth panel). These results suggest that fractions 1 and 5 are the PM- and endosome-rich fractions, respectively. When these fractions were employed in the cell-free γ-secretase assay, we found that the peak height of AICDϵ51 relative to that of AICDϵ49 was larger in the endosome-rich fraction than in the PM-rich fraction (Figure 3C). In contrast, the peak height of AICDϵ49 relative to that of AICDϵ51 was higher in the PM-rich fraction than the endosome-rich fraction (Figure 3C). Similarly, using membrane fractions from HeLa cells, we found that AICDϵ49 was the dominant product in PM-rich fractions, whereas AICDϵ51 was the main product in endosome-rich fractions. These results indicate that the precision of ϵ-cleavage differs on PM and endosomes. Specifically, cleavage at ϵ49, which lies deeper inside the transmembrane domain, tends to occur more on PM than endosomes, whereas the opposite is true for cleavage at ϵ51, which lies closer to the cytosolic side and the interface between transmembrane and intracellular domains.

The Precision of ϵ-Cleavage Is Affected by pH. Our results show that the precision of cleavage at the ϵ-site changes drastically upon inhibition of endocytosis and is affected by the subcellular location. The process of cleavage by PS/γ-secretase may therefore change according to the surrounding conditions. For this reason, we examined whether changing the pH during the cell-free γ-secretase assay affects the level and precision of ϵ- and γ-cleavage. IP-MS showed that, when

Table 1: Amino Acid Sequences of AICDϵ49 and AICDϵ51 Species

MW (obsd)	species	sequence	MW (calcd)
5911	AICDϵ49	V^{646}MLKKKQYTSIHHGVVEVDAAVTPEERHLSKMQQNGYENPTYKFFEQMQN^{695}	5910.7
5680	AICDϵ51	L^{648} KKKQYTSIHHGVVEVDAAVTPEERHLSKMQQNGYENPTYKFFEQMQN^{695}	5680.4

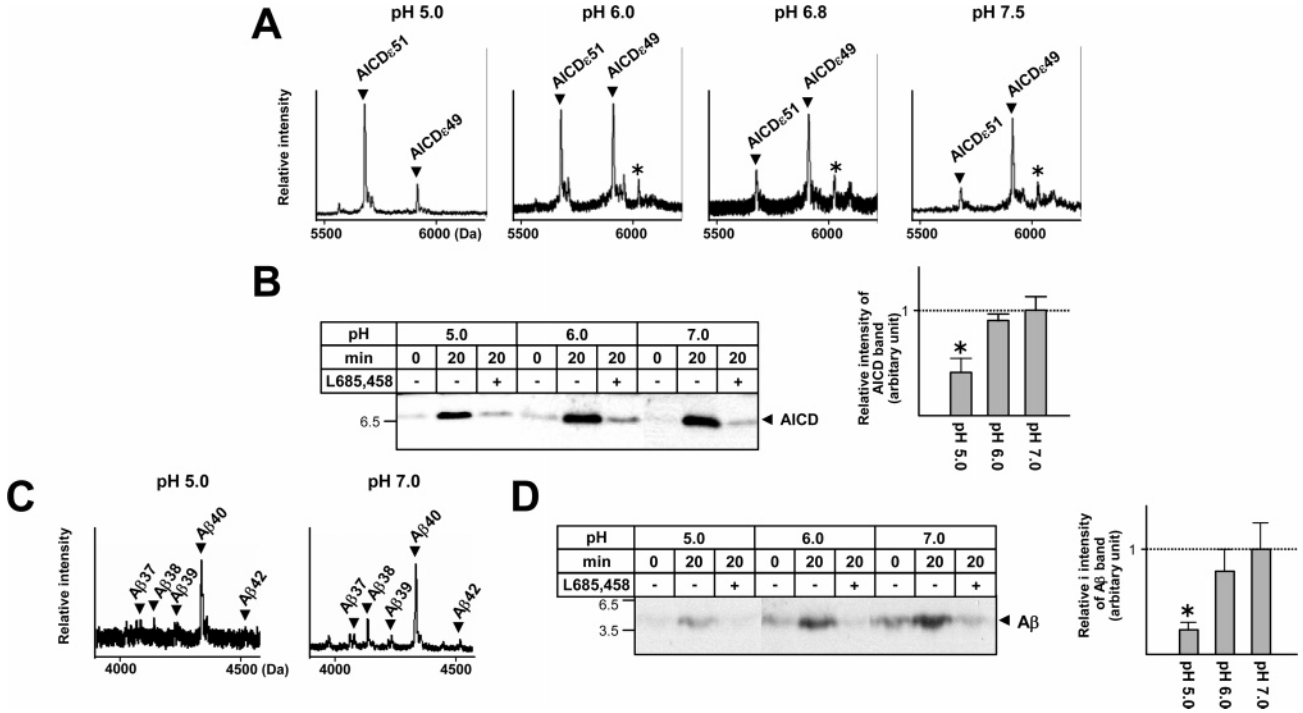

FIGURE 4: Effects of pH on ϵ- and γ-cleavage. (A) Mass spectra of AICD generated in the cell-free assay at pHs between 7.5 and 5.0. CMFs from βAPP sw-expressing K293 cells were resuspended in reaction buffer at the indicated pH. Asterisks indicate AICDϵ48 species. (B) The level of AICDs generated at various pHs. The cell-free incubation was performed in the presence of either L685,458 or vehicle alone (DMSO) (left panel). The asterisk indicates that the intensity of the AICD band at pH 5.0 was statistically lower than those at pH 6.0 and 7.0 ($P < 0.01$ by Student's *t*-test). (C) Mass spectra of Aβ generated in the cell-free assay at pH 5.0 and 7.0. (D) The level of Aβ generated at various pHs and in the presence of L685,458 or vehicle control (DMSO). The asterisk indicates statistical significance ($P < 0.01$ by Student's *t*-test). In (A) and (C) and the left panels of (B) and (D), the results are representative of more than three independent experiments. In the right panels of (B) and (D), the results indicate the means ± standard deviations from at least triplicate determinations.

we changed the buffer pH from 7.5 to 5.0, the relative cleavage efficiency at the ϵ49 and ϵ51 sites changed (Figure 4A). The more acidic the pH, the higher the AICDϵ51 peak became, demonstrating that the pH affects cleavage at the ϵ-site. Immunoblotting also showed that lowering the pH to 5.0 decreased the amount of AICD produced, indicating a reduction in the total amount of cleavage at the ϵ-site (Figure 4B). De novo AICD production was almost completely suppressed by an inhibitor of PS-dependent γ-secretase (L685,458) at various pHs. Therefore, the AICD production that we observed was mostly due to proteolysis by PS-dependent γ-secretase (Figure 4B). These results indicate that alteration of the pH affects both the precision and the level of ϵ-site cleavage. We also studied the effect of pH on the precision and amount of γ-site cleavage. As shown in Figure 4C, we could not detect any ϵ-cleavage-like changes in the precision of γ-cleavage. Also, lowering the pH to 5.0 caused a reduction in the total amount of de novo Aβ production (Figure 4D). Therefore, lowering the pH reduced the level of cleavage at both the γ- and ϵ-sites. Collectively, these results show that the pH in the cell-free assay affects the precision of cleavage at the ϵ-site.

DISCUSSION

In this study, we investigated intramembrane proteolysis of βAPP and demonstrated dynamic changes in the precision of cleavage by the PS/γ-secretase. Using a cell-free γ-secretase assay, we showed that the precision of ϵ-site cleavage changes depending on the subcellular location and pH. These results suggest that the precision of cleavage by the PS/γ-secretase complex can be regulated physiologically.

Inhibition of endocytosis also induced a change in the precision of ϵ-cleavage, suggesting that the function of PS/γ-secretase is related to endocytosis. The precision of ϵ-cleavage on PM and endosomes differs, demonstrating that the function of PS/γ-secretase may be heterogeneous in cells. It is unlikely that the change in precision of ϵ-cleavage observed in this study is due to differences in the thickness of PM and endosome membranes because very similar changes were caused by altering the pH in the cell-free assay. Moreover, our results suggest that the precision of ϵ-cleavage is more dynamic than that of γ-cleavage. Therefore, our results can be explained by (i) additional physiological factors that interact with the active PS/γ-secretase complex or (ii) altered substrate recognition/access at different pH conditions that exist at the plasma membrane and endosomes.

Because the PS/γ-secretase complex mediates both γ- and ϵ-cleavages in the transmembrane domain of βAPP (*2*), one might predict that the processes of γ- and ϵ-cleavage would behave the same. Previous results have shown, however, that the effects of PS mutations on the relative levels of γ42 and

ϵ-site cleavages do not always correlate (*17*). Furthermore, in the current study, we showed that the precision of ϵ- and γ-site cleavages on PM and endosomes did not change in parallel. Our results support the hypothesis that the ϵ-cleavage process is distinct from that of the γ-cleavage, although both occur on the same transmembrane domain and are mediated by the same PS-dependent γ-secretases.

Recent reports have described the existence of several long Aβ species that are thought to be membrane-bound remnants from ϵ-cleavage of CTF stubs (*35*−*37*). Also, it has been reported that there is an association between the cleavages at ϵ51 and at γ42, which are types of ϵ- and γ-site cleavages, respectively (*16*). These findings indicate that there is a time-dependent relationship between γ- and ϵ-cleavages, namely, that γ-cleavage follows ϵ-cleavage (*36*, *37*). If this is generally true, de novo AICD and Aβ is generated from distinct substrates in our cell-free assay; in other words, AICDs is generated from CTF stubs of βAPP, whereas Aβ must be generated from long and membrane-bound Aβ. Otherwise, our results suggest that the process determining the precision of ϵ-cleavage is distinct from that for the γ-cleavage. Thus, it appears that the time-dependent association between γ- and ϵ-cleavages either is not dominant but rather simply reflects the rate of each cleavage under physiological conditions.

In our cell-free assay, conditions mimicking physiological cell functions (i.e., changes in subcellular location, endocytosis, and pH) affected the efficiency of cleavage at ϵ49 and ϵ51; however, we could not find any consistent correlations between relative peak heights of AICDϵ48 and those of AICDϵ49 or AICDϵ51, even though AICDϵ48 was one of the major species.

In summary, we demonstrate here that the precision of ϵ-cleavage of βAPP changes depending on endocytotic function. In future studies, we will examine whether similar changes in the precision of PS-mediated cleavage in the TM-C also occur for other substrates, such as Notch-1.

ACKNOWLEDGMENT

We thank Drs. Harald Steiner, Masaki Nishimura, Maho Morishima-Kawashima, and Yasuo Ihara for critically reading the manuscript. We also thank Drs. Sandra L. Schmid and Takeshi Baba for providing Dyn-1 K44A-expressing HeLa cells.

SUPPORTING INFORMATION AVAILABLE

Four figures indicating that (i) inhibition of endocytosis by bafilomycin A1 treatment caused a drastic change of ϵ-cleavage precision, (ii) the relative ratio of the AICDϵ49 peak height to that of AICDϵ51 semiquantitatively correlated with the relative amount of each AICD species, and (iii) wt βAPP as well as βAPP sw caused the drastic change in the precision of ϵ-cleavage. This material is available free of charge via the Internet at http://pubs.acs.org.

REFERENCES

1. Selkoe, D., and Kopan, R. (2003) Notch and presenilin: regulated intramembrane proteolysis links development and degeneration, *Annu. Rev. Neurosci. 26*, 565−597.
2. Haass, C. (2004) Take five-BACE and the gamma-secretase quartet conduct Alzheimer's amyloid beta-peptide generation, *EMBO J. 23*, 483−488.
3. Okochi, M., Steiner, H., Fukumori, A., Tanii, H., Tomita, T., Tanaka, T., Iwatsubo, T., Kudo, T., Takeda, M., and Haass, C. (2002) Presenilins mediate a dual intramembranous gamma-secretase cleavage of Notch-1, *EMBO J. 21*, 5408−5416.
4. Lammich, S., Okochi, M., Takeda, M., Kaether, C., Capell, A., Zimmer, A. K., Edbauer, D., Walter, J., Steiner, H., and Haass, C. (2002) Presenilin-dependent intramembrane proteolysis of CD44 leads to the liberation of its intracellular domain and the secretion of an Abeta-like peptide, *J. Biol. Chem. 277*, 44754−44759.
5. Okochi, M., Fukumori, A., Jiang, J., Itoh, N., Kimura, R., Steiner, H., Haass, C., Tagami, S., and Takeda, M. (2006) Secretion of the Notch-1 Abeta-like peptide during Notch signaling, *J. Biol. Chem.* (in press).
6. Sastre, M., Steiner, H., Fuchs, K., Capell, A., Multhaup, G., Condron, M. M., Teplow, D. B., and Haass, C. (2001) Presenilin-dependent gamma-secretase processing of beta-amyloid precursor protein at a site corresponding to the S3 cleavage of Notch, *EMBO Rep. 2*, 835−841.
7. Chen, F., Gu, Y., Hasegawa, H., Ruan, X., Arawaka, S., Fraser, P., Westaway, D., Mount, H., and St George-Hyslop, P. (2002) Presenilin 1 mutations activate gamma 42-secretase but reciprocally inhibit epsilon-secretase cleavage of amyloid precursor protein (APP) and S3-cleavage of notch, *J. Biol. Chem. 277*, 36521−36526.
8. Yu, C., Kim, S. H., Ikeuchi, T., Xu, H., Gasparini, L., Wang, R., and Sisodia, S. S. (2001) Characterization of a presenilin-mediated amyloid precursor protein carboxyl-terminal fragment gamma. Evidence for distinct mechanisms involved in gamma-secretase processing of the APP and Notch1 transmembrane domains, *J. Biol. Chem. 276*, 43756−43760.
9. Gu, Y., Misonou, H., Sato, T., Dohmae, N., Takio, K., and Ihara, Y. (2001) Distinct intramembrane cleavage of the beta-amyloid precursor protein family resembling gamma-secretase-like cleavage of Notch, *J. Biol. Chem. 276*, 35235−35238.
10. Weidemann, A., Eggert, S., Reinhard, F. B., Vogel, M., Paliga, K., Baier, G., Masters, C. L., Beyreuther, K., and Evin, G. (2002) A novel epsilon-cleavage within the transmembrane domain of the Alzheimer amyloid precursor protein demonstrates homology with Notch processing, *Biochemistry 41*, 2825−2835.
11. Selkoe, D. J. (2001) Alzheimer's disease: genes, proteins, and therapy, *Physiol. Rev. 81*, 741−766.
12. Weggen, S., Eriksen, J. L., Das, P., Sagi, S. A., Wang, R., Pietrzik, C. U., Findlay, K. A., Smith, T. E., Murphy, M. P., Bulter, T., Kang, D. E., Marquez-Sterling, N., Golde, T. E., and Koo, E. H. (2001) A subset of NSAIDs lower amyloidogenic Abeta42 independently of cyclooxygenase activity, *Nature 414*, 212−216.
13. Kukar, T., Murphy, M. P., Eriksen, J. L., Sagi, S. A., Weggen, S., Smith, T. E., Ladd, T., Khan, M. A., Kache, R., Beard, J., Dodson, M., Merit, S., Ozols, V. V., Anastasiadis, P. Z., Das, P., Fauq, A., Koo, E. H., and Golde, T. E. (2005) Diverse compounds mimic Alzheimer disease-causing mutations by augmenting Abeta42 production, *Nat. Med. 11*, 545−550.
14. Lazarov, O., Robinson, J., Tang, Y. P., Hairston, I. S., Korade-Mirnics, Z., Lee, V. M., Hersh, L. B., Sapolsky, R. M., Mirnics, K., and Sisodia, S. S. (2005) Environmental enrichment reduces Abeta levels and amyloid deposition in transgenic mice, *Cell 120*, 701−713.
15. Sato, T., Dohmae, N., Qi, Y., Kakuda, N., Misonou, H., Mitsumori, R., Maruyama, H., Koo, E. H., Haass, C., Takio, K., Morishima-Kawashima, M., Ishiura, S., and Ihara, Y. (2003) Potential link between amyloid beta-protein 42 and C-terminal fragment gamma 49−99 of beta-amyloid precursor protein, *J. Biol. Chem. 278*, 24294−24301.
16. Funamoto, S., Morishima-Kawashima, M., Tanimura, Y., Hirotani, N., Saido, T. C., and Ihara, Y. (2004) Truncated carboxyl-terminal fragments of beta-amyloid precursor protein are processed to amyloid beta-proteins 40 and 42, *Biochemistry 43*, 13532−13540.
17. Moehlmann, T., Winkler, E., Xia, X., Edbauer, D., Murrell, J., Capell, A., Kaether, C., Zheng, H., Ghetti, B., Haass, C., and Steiner, H. (2002) Presenilin-1 mutations of leucine 166 equally affect the generation of the Notch and APP intracellular domains independent of their effect on Abeta 42 production, *Proc. Natl. Acad. Sci. U.S.A. 99*, 8025−8030.
18. Iwatsubo, T. (2004) The gamma-secretase complex: machinery for intramembrane proteolysis, *Curr. Opin. Neurobiol. 14*, 379−383.
19. Yu, G., Nishimura, M., Arawaka, S., Levitan, D., Zhang, L., Tandon, A., Song, Y. Q., Rogaeva, E., Chen, F., Kawarai, T.,

Supala, A., Levesque, L., Yu, H., Yang, D. S., Holmes, E., Milman, P., Liang, Y., Zhang, D. M., Xu, D. H., Sato, C., Rogaev, E., Smith, M., Janus, C., Zhang, Y., Aebersold, R., Farrer, L. S., Sorbi, S., Bruni, A., Fraser, P., and St. George-Hyslop, P. (2000) Nicastrin modulates presenilin-mediated notch/glp-1 signal transduction and betaAPP processing, *Nature 407*, 48−54.

20. Francis, R., McGrath, G., Zhang, J., Ruddy, D. A., Sym, M., Apfeld, J., Nicoll, M., Maxwell, M., Hai, B., Ellis, M. C., Parks, A. L., Xu, W., Li, J., Gurney, M., Myers, R. L., Himes, C. S., Hiebsch, R., Ruble, C., Nye, J. S., and Curtis, D. (2002) aph-1 and pen-2 are required for Notch pathway signaling, gamma-secretase cleavage of betaAPP, and presenilin protein accumulation, *Dev. Cell 3*, 85−97.
21. Wilson, C. A., Doms, R. W., Zheng, H., and Lee, V. M. (2002) Presenilins are not required for A beta 42 production in the early secretory pathway, *Nat. Neurosci. 5*, 849−855.
22. Lai, M. T., Crouthamel, M. C., DiMuzio, J., Pietrak, B. L., Donoviel, D. B., Bernstein, A., Gardell, S. J., Li, Y. M., and Hazuda, D. (2006) A presenilin-independent aspartyl protease prefers the gamma-42 site cleavage, *J. Neurochem. 96*, 118−125.
23. Okochi, M., Ishii, K., Usami, M., Sahara, N., Kametani, F., Tanaka, K., Fraser, P. E., Ikeda, M., Saunders, A. M., Hendriks, L., Shoji, S. I., Nee, L. E., Martin, J. J., Van Broeckhoven, C., St. George-Hyslop, P. H., Roses, A. D., and Mori, H. (1997) Proteolytic processing of presenilin-1 (PS-1) is not associated with Alzheimer's disease with or without PS-1 mutations, *FEBS Lett. 418*, 162−166.
24. Okochi, M., Eimer, S., Bottcher, A., Baumeister, R., Romig, H., Walter, J., Capell, A., Steiner, H., and Haass, C. (2000) A loss of function mutant of the presenilin homologue SEL-12 undergoes aberrant endoproteolysis in *Caenorhabditis elegans* and increases abeta 42 generation in human cells, *J. Biol. Chem. 275*, 40925−40932.
25. Steiner, H., Romig, H., Pesold, B., Philipp, U., Baader, M., Citron, M., Loetscher, H., Jacobsen, H., and Haass, C. (1999) Amyloidogenic function of the Alzheimer's disease-associated presenilin 1 in the absence of endoproteolysis, *Biochemistry 38*, 14600−14605.
26. Damke, H., Baba, T., Warnock, D. E., and Schmid, S. L. (1994) Induction of mutant dynamin specifically blocks endocytic coated vesicle formation, *J. Cell Biol. 127*, 915−934.
27. Mizutani, T., Taniguchi, Y., Aoki, T., Hashimoto, N., and Honjo, T. (2001) Conservation of the biochemical mechanisms of signal transduction among mammalian Notch family members, *Proc. Natl. Acad. Sci. U.S.A. 98*, 9026−9031.
28. Pinnix, I., Musunuru, U., Tun, H., Sridharan, A., Golde, T., Eckman, C., Ziani-Cherif, C., Onstead, L., and Sambamurti, K. (2001) A novel gamma-secretase assay based on detection of the putative C-terminal fragment-gamma of amyloid beta protein precursor, *J. Biol. Chem. 276*, 481−487.
29. McLendon, C., Xin, T., Ziani-Cherif, C., Murphy, M. P., Findlay, K. A., Lewis, P. A., Pinnix, I., Sambamurti, K., Wang, R., Fauq, A., and Golde, T. E. (2000) Cell-free assays for gamma-secretase activity, *FASEB J. 14*, 2383−2386.
30. Okochi, M., Walter, J., Koyama, A., Nakajo, S., Baba, M., Iwatsubo, T., Meijer, L., Kahle, P. J., and Haass, C. (2000) Constitutive phosphorylation of the Parkinson's disease associated alpha-synuclein, *J. Biol. Chem. 275*, 390−397.
31. Chyung, J. H., and Selkoe, D. J. (2003) Inhibition of receptor-mediated endocytosis demonstrates generation of amyloid beta-protein at the cell surface, *J. Biol. Chem. 278*, 51035−51043.
32. Wolfe, M. S., Xia, W., Ostaszewski, B. L., Diehl, T. S., Kimberly, W. T., and Selkoe, D. J. (1999) Two transmembrane aspartates in presenilin-1 required for presenilin endoproteolysis and gamma-secretase activity, *Nature 398*, 513−517.
33. Kimberly, W. T., and Wolfe, M. S. (2003) Identity and function of gamma-secretase, *J. Neurosci. Res. 74*, 353−360.
34. Stevens, T. H., and Forgac, M. (1997) Structure, function and regulation of the vacuolar (H+)-ATPase, *Annu. Rev. Cell Dev. Biol. 13*, 779−808.
35. Zhao, G., Mao, G., Tan, J., Dong, Y., Cui, M. Z., Kim, S. H., and Xu, X. (2004) Identification of a new presenilin-dependent zeta-cleavage site within the transmembrane domain of amyloid precursor protein, *J. Biol. Chem. 279*, 50647−50650.
36. Qi-Takahara, Y., Morishima-Kawashima, M., Tanimura, Y., Dolios, G., Hirotani, N., Horikoshi, Y., Kametani, F., Maeda, M., Saido, T. C., Wang, R., and Ihara, Y. (2005) Longer forms of amyloid beta protein: implications for the mechanism of intramembrane cleavage by gamma-secretase, *J. Neurosci. 25*, 436−445.
37. Zhao, G., Cui, M. Z., Mao, G., Dong, Y., Tan, J., Sun, L., and Xu, X. (2005) gamma-Cleavage is dependent on zeta-cleavage during the proteolytic processing of amyloid precursor protein within its transmembrane domain, *J. Biol. Chem. 280*, 37689−37697.

BI052412W